Application of the ordered logit model to optimising Frangi filter parameters for segmentation of perivascular spaces

Available online at www.sciencedirect.com

ScienceDirect

Procedia Computer Science 90 (2016) 61 – 67

Procedia Computer Science

International Conference On Medical Imaging Understanding and Analysis 2016, MIUA 2016, 6-8 July 2016, Loughborough, UK

Application of the ordered logit model to optimising Frangi filter parameters for segmentation of perivascular spaces

Lucia Ballerini*[a,c], Ruggiero Lovreglio[b], Maria del C. Valdés Hernández[a,c], Victor Gonzalez-Castro[a,c], Susana Muñoz Maniega[a,c], Enrico Pellegrini[a], Mark E. Bastin[a,c], Ian J. Deary[c,d], Joanna M. Wardlaw[a,c]

[a]*Department of Neuroimaging Sciences, University of Edinburgh, UK*
[b]*Department of Civil and Environmental Engineering, University of Auckland, NZ*
[c]*Centre for Cognitive Ageing and Cognitive Epidemiology, University of Edinburgh, UK*
[d]*Department of Psychology, University of Edinburgh, UK*

Abstract

Segmentation of perivascular spaces (PVS) from brain magnetic resonance images (MRI) is important for understanding the brain's lymphatic system and its relationship with neurological diseases. The Frangi filter might be a valuable tool for this purpose. However, its parameters need to be adjusted in response to the variability in the scanner's parameters and study protocols. Knowing the neuroradiological ratings of the PVS, we used the ordered logit model to optimise Frangi filter parameters. The PVS volume obtained significantly and strongly correlated with neuroradiological assessments (Spearman's ρ=0.75, $p < 0.001$), suggesting that the ordered logit model could be a good alternative to conventional optimisation frameworks for segmenting PVS on MRI.

Peer-review under responsibility of the Organizing Committee of MIUA 2016

Keywords: ordered logit model; perivascular spaces; Frangi filter; brain; MRI

1. Introduction

Perivascular spaces (PVS), also known as Virchow-Robin spaces, are small tubular structures that look round or linear depending on the viewing plane (see Fig. 1 (a)), on brain magnetic resonance imaging (MRI) with intensities close to those of the cerebrospinal fluid [1,2]. When associated with ageing, cerebral small vessel disease (SVD), cognitive impairment, and inflammation [3], they are mainly found in four brain regions: midbrain and pons, corpus striatum, hippocampi and centrum semiovale [1]. Most studies use visual rating scales to assess PVS, but these have limitations

* Corresponding author. Tel.: +44-131-4659529
E-mail address: lucia.ballerini@ed.ac.uk

Peer-review under responsibility of the Organizing Committee of MIUA 2016
doi:10.1016/j.procs.2016.07.011

and are prone to observer variation, specially in the centrum semiovale (CS), due to the coexistence of PVS with other neuroradiological features of SVD that confound their identification in this region.

Efforts have been made to computationally assess PVS[4,5]. Recent semi-automatic methods are based on thresholding and requires user intervention either for the choice of parameters or for manual editing of the resulting masks[6,7]. One of the most promising approaches proposed for PVS automatic segmentation uses the Frangi filter[8] parameterised through a random forest scheme that learns discriminative PVS characteristics from manually segmented ground truth on MR images acquired at 7T[9,10]. However, in reality, MRI in clinical research and practice is mostly done in scanners with field strengths of 1.5T or 3T, and the reference standard available are visual ratings done by neuroradiologists, all that makes the learning-based approach proposed by Park et al.[10] unsuitable for being widely applicable.

We propose a novel application of the ordered logit model, usually used in statistics as a regression model for ordinal dependent variables, as this model provides a good estimate for capturing the sources of influence that explain the ordinal dependent variables (i.e. in this case the PVS visual rating scores) considering the uncertainty (i.e. subjectivity, inter-observer variability) in the measurement of such data[11]. We use this model to estimate the parameters of the Frangi filter[8] to obtain the maximum likelihood of a vessel-like structure to be a PVS in the CS by also estimating the count of PVS that most probably fall in the class correspondent to the category given by the neuroradiologist in this brain region.

2. Methods

2.1. Visual Ratings of PVS

PVS were assessed by an experienced neuroradiologist using the visual rating scale developed by Potter et al.[12], which rates the PVS burden separately on T2-weighted MRI in three major anatomical brain regions (i.e. midbrain, basal ganglia and centrum semiovale) as 0 (no PVS), 1 (mild; 1-10 PVS), 2 (moderate; 11-20 PVS), 3 (frequent; 21-40 PVS) or 4 (severe; >40 PVS). Examples of each rating category for the centrum semiovale are shown in Fig. 1 (b).

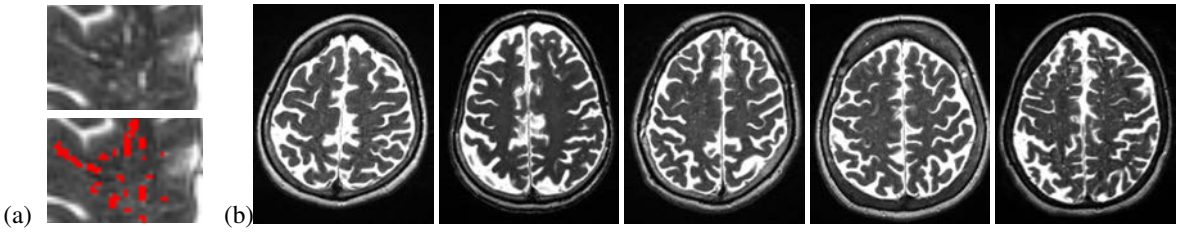

Fig. 1. (a) Enlarged area of an axial slice with PVS. (b) Examples of the PVS rating categories (0 to 4) in the centrum semiovale

2.2. Selection of the Region of Interest

Automatic brain, cerebrospinal fluid (CSF) and normal-appearing white matter extraction were performed on T1-weighted MRI using optiBET[13] and FSL-FAST[14] respectively. All subcortical structures were segmented, also automatically, using other tools from the FMRIB Software Library (FSL) and an age-relevant template as per the pipeline described elsewhere[15]. After identifying the lateral ventricles as the CSF-filled structures with boundaries with the subcortical structures, the CS was identified as the region of normal-appearing white matter, superior to the lateral ventricles, present in each of the cerebral hemispheres under the cerebral cortex. T1-weighted sequence and CS region were linearly registered to the T2-weighted[16] as the latter is the sequence where PVS are assessed[5].

2.3. Segmentation of PVS

The MRI volumes (voxel dimensions $1mm \times 1mm \times 2mm$) were resliced to make $1mm$ isotropic voxels using linear interpolation. As per Frangi et. al[8], the "vesselness" $F(v)$ of a voxel v at scale s was calculated as:

$$F_s(v) = \begin{cases} 0 & \text{if } \lambda_2 \geq 0 \text{ or } \lambda_3 \geq 0, \\ (1 - e^{-\frac{R_A^2}{2\alpha^2}}) \cdot e^{-\frac{R_B^2}{2\beta^2}} \cdot (1 - e^{-\frac{S^2}{2c^2}}) & \text{otherwise}, \end{cases} \quad (1)$$

where λ_1, λ_2 and λ_3 are eigenvalues of the Hessian matrix, $R_A = |\lambda_2|/|\lambda_3|$, $R_B = |\lambda_1|/(|\lambda_2\lambda_3|)^{1/2}$, $S = (\lambda_1^2 + \lambda_2^2 + \lambda_3^2)^{1/2}$, and α, β, c are used defined parameters. Given a set of scales $s \in [s_{min}, s_{max}]$, the responses were combined as

$$F(v) = \max_s F_s(v) \quad (2)$$

The voxels having F(v) larger than a threshold t were kept. PVS were identified using 3D connected component analysis as the tubular structures with lengths between 3 and $50mm$[5,7]. The Frangi filter parameters α, β, c, the scales s_{min}, s_{max} and the threshold t were the parameters needed to be optimized.

2.4. Ordered Logit Model

An ordered logit model has been used to simulate the relationship between the number of PVS and the rating categories taking into account the uncertainty in the measurements. This modelling approach provides a relevant methodology for capturing the sources of influence (independent variables) that explain an ordinal variable (dependent variable) taking into account the measurement uncertainty of such data[11]. The ordered logit model defines the relationship between the rating class (y) and the PVS number (x) by using a latent continuous variable ($y^\star$) defined in an one-dimensional space characterized by threshold points ($\mu_0, \ldots, \mu_4$) as described in equation:

$$\begin{array}{l} y^\star = \beta x + \epsilon, \quad \epsilon \sim L(\mu|\sigma), \quad \mu = 0, \quad \sigma = \pi/\sqrt{3} \\ \text{y} = 0 \quad \textit{if} \quad -\infty < y^\star \leq \mu_0 \\ \text{y} = 1 \quad \textit{if} \quad \mu_0 < y^\star \leq \mu_1 \\ \text{y} = 2 \quad \textit{if} \quad \mu_1 < y^\star \leq \mu_2 \\ \text{y} = 3 \quad \textit{if} \quad \mu_2 < y^\star \leq \mu_3 \\ \text{y} = 4 \quad \textit{if} \quad \mu_3 < y^\star \leq \infty \end{array} \quad (3)$$

where β and μ_i are parameters to be estimated, ϵ is the error component which has a logistic random distribution with expected value equal to 0 and variance equal to $\pi/\sqrt{3}$, that accounts for the measurement error.

Since $y^\star$ is not a deterministic quantity, it is only possible to define the probability to belong to each class:

$$P(y = j|\bar{x}) = P(\mu_{j-1} < \bar{y}^\star \leq \mu_j) = L(\mu_j - \beta\bar{x}) - L(\mu_{j-1} - \beta\bar{x}), \quad j = 0, \ldots, 4 \quad (4)$$

where L is the logistic cumulative distribution function.

This model has been calibrated maximizing a likelihood function based on a synthetic dataset generated in 2 steps. In the first step 1000 numbers of PVS count have been generated using a log-normal distribution (median:15, SD:1) to represent the PVS population. In the second step a rating class from 0 to 4 (0 = none, 1 = 1 − 10, 2 = 11 − 20, 3 = 21 − 40, 4 = > 40 PVS) has been assigned to each generated number. The estimated parameters are $\beta = 0.514$, $\mu_0 = -2.840$, $\mu_1 = 5.708$, $\mu_2 = 10.497$, $\mu_3 = 20.040$, and the model is illustrated in Fig. 2

2.5. Parameter Optimization

To optimize the segmentation parameters, a log-likelihood function has been defined as the function to maximize. This function can be calculated for each set of parameters (α, β, c, s_{min}, s_{max} and t). With the procedure described in Sec. 2.3, using these parameters, we obtained a PVS binary mask. For each slice we calculated the PVS density as the area of the PVS mask divided by the area of the CS mask (obtained as described in Sec. 2.2). We automatically selected in the CS the slice with higher density of PVS. This slice corresponds to the representative slice having the highest number of PVS chosen by the radiologist for assessing the visual ratings[12]. The count of PVS in this slice has been derived automatically with 2D connected component labelling. From the count of PVS ($x_i(\alpha, \beta, c, s_{min}, s_{max}, t)$) for each i case we obtained the probabilities of each i case to belong to the five rating classes ($P(y = j|x_i)$, $j = 0, \ldots, 4$)

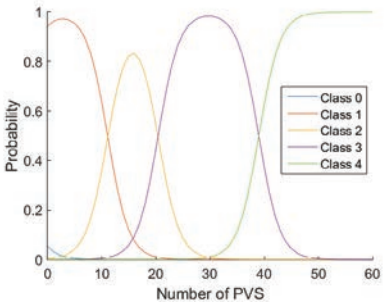

Fig. 2. Estimated ordered logit model

using the ordered logit model. The PVS visual rating category provided by an expert radiologist is then used to select a probability for each i case ($\bar{P}_i$). The sum of the logarithms of these selected probabilities is the log-likelihood function to maximize:

$$LogL(\alpha, \beta, c, s_{min}, s_{max}, t) = \sum_{i=1}^{N} log(\bar{P}_i) \tag{5}$$

where N is the number of cases. The optimization process is illustrated in Fig. 3. The ranges of the parameters that undergo the optimization process has been defined as in Table 1.

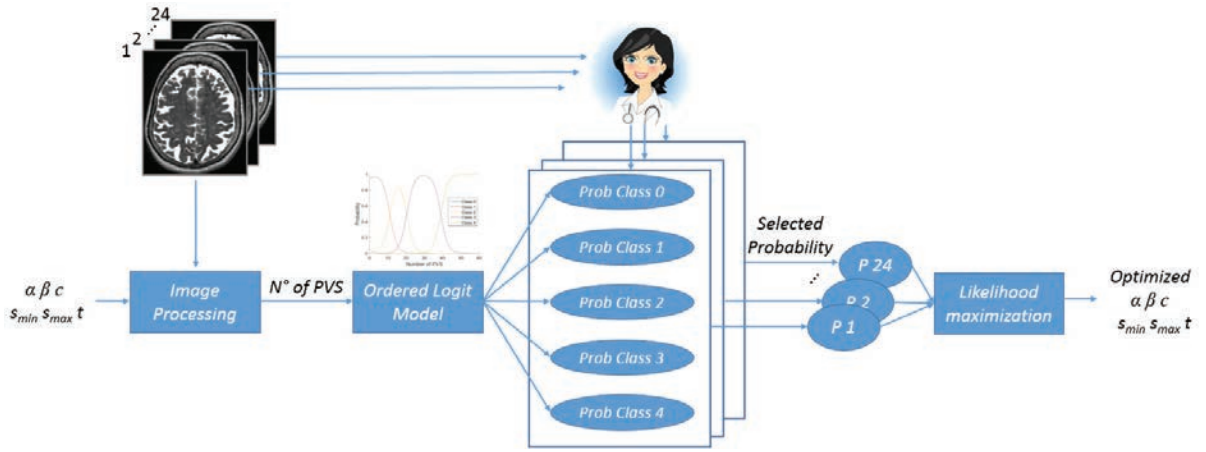

Fig. 3. Optimization approach

Table 1. Range of the segmentation parameters to optimize

	α	β	c	s_{min}	s_{max}	t
min value	0.3	0.3	300	0.1	0.1	0.2
max value	0.7	0.7	700	0.5	1.0	0.4
increment	0.1	0.1	100	0.1	0.1	0.05

The usual drawback of optimization processes is the computational time necessary to simultaneously optimize multiple parameters. Indeed, each log-likelihood function evaluation implies filtering all the training samples using eq. (1), which may become critical in this 3D case. To reduce the computational time, in this research contribution, we performed a series of optimization steps, such that in each step the optimization is limited to subsets of parameters. The optimal parameters obtained in the first step have been kept constant to optimize the remaining ones.

3. Experiments and Results

For developing and optimizing the segmentation approach, the imaging datasets of 24 subjects were chosen from a sample of the Lothian Birth Cohort 1936 Study (LBC1936) (http://www.lothianbirthcohort.ed.ac.uk/). The number of training images for each rating score have been chosen to reflect the distribution in the full dataset. To evaluate the new method, we applied the optimized segmentation procedure described in Sec. 2.3 to 60 patients of the same older person study. Visual ratings of PVS was available for all these cases (Table 2).

Table 2. Distribution of the PVS visual ratings in the training and test dataset.

PVS rating	0	1	2	3	4	Total
Training images	1	5	8	6	4	24
Test images	0	11	22	18	9	60

Segmentation procedures are commonly evaluated assessing the voxel-wise spatial agreement between two binary masks, one obtained by the automatic method and a manual one. In our case, the manual segmentation of PVS is not available, as it will be a very tedious and time consuming task to manually annotate these tiny structures in a reasonable size dataset. For this reason we could not report accuracy values. Quantitative comparison with other methods[4,6,7] is also unfeasible as they have been applied to MR images having different resolution, acquired using different protocols in different cohorts. Volume rendering of the segmented PVS for the subjects of 4 rating categories (1 to 4) of Fig. 1 is shown in Fig. 4 for visual qualitative evaluation.

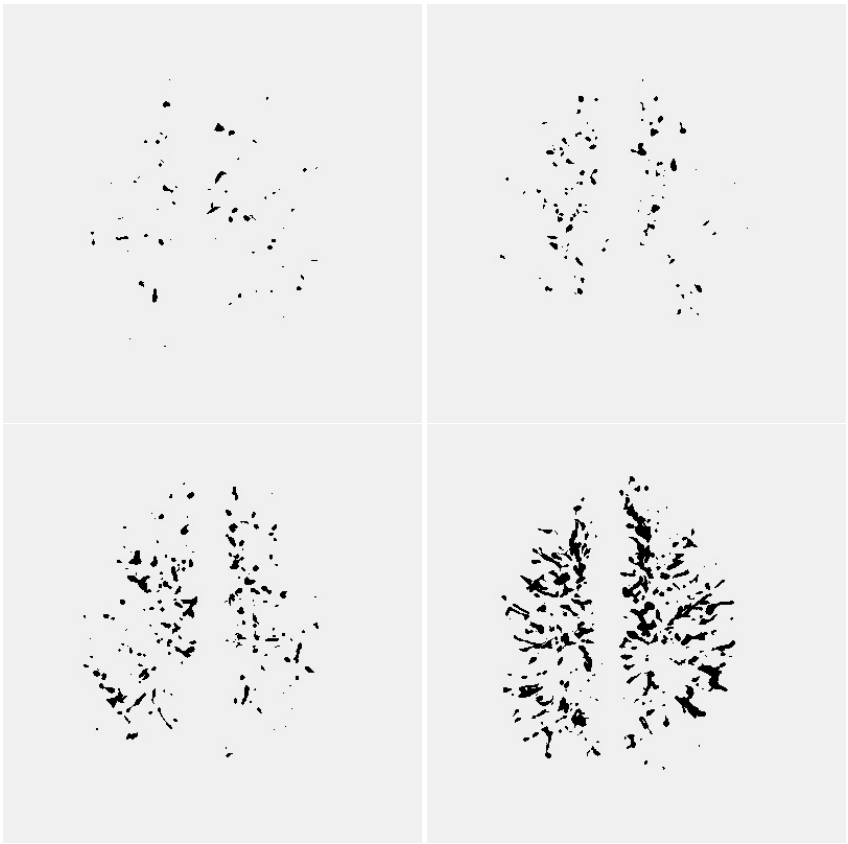

Fig. 4. Volume rendering of segmented PVS for 4 subjects of Fig. 1 with rating categories 1 to 4

We tested associations between segmentation results of the 60 test cases and their rating scores using Spearman's ρ (statistical analysis were performed using MATLAB Robust correlation toolbox[17]). The PVS volume and count

strongly correlated with visual rating scores (Spearman's $\rho = 0.75$ and 0.69, respectively, both $p < 0.001$). Scatter plots of these associations are shown in Fig. 5.

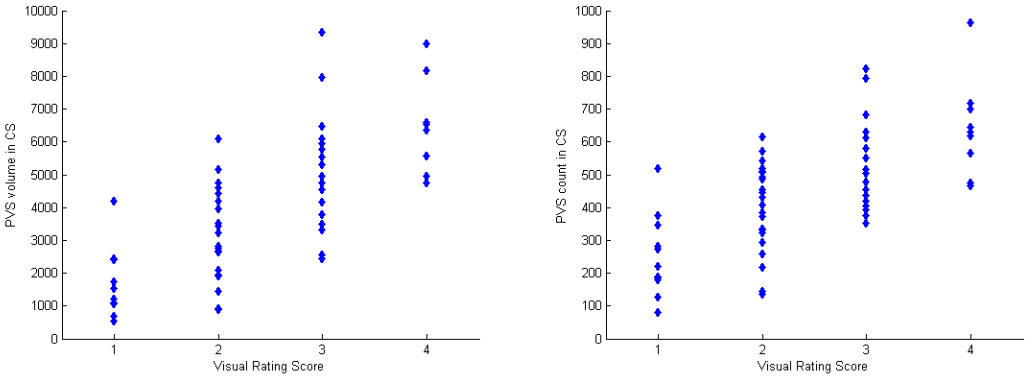

Fig. 5. Associations between PVS computational total volume and count vs. PVS visual rating scores in centrum semiovale (CS) region.

4. Conclusions

We presented an automatic method for 3D segmentation of PVS in conventional MRI. Thanks to the 3D Frangi filter that enhances and captures the 3D geometrical shape of PVS, this method shows promise for allowing identifying and quantifying PVS that run both longitudinally and transversally in the CS, avoiding the double-counting limitations of slice-based methods. The novelty of this work is the fact that the ordered logit model allows to use the visual ratings for segmentation optimization in absence of alternative computational ground truth. The ordered logit model could deal with the measurement uncertainty and the unequal class intervals of the rating scores.

The automatically segmented PVS count and volume agree with visual ratings. The method is fully automatic and therefore free from inter- and intra-rater variability. However, much more testing is required in a wider range of subjects including those with high burden of other ageing and neuroinflammation features such as patients with stroke or multiple sclerosis. The quantitative assessment of PVS volume and count is more suitable for longitudinal studies than visual ratings, that tend to be susceptible to ceiling/flooring effects. The accurate segmentation of PVS will allow the analysis of their spatial distribution, orientation and density. Moreover it will enable the study of the spatial and volumetric relationships of PVS with other markers of SVD, e.g. acute lacunar infarcts, white matter hyperintensities, lacunes, and microbleeds, including potentially in longitudinal studies and in relation to measures of cerebral blood brain barrier permeability, perfusion and cerebrovascular reactivity. Quantitative measurements will better characterize the severity of PVS in ageing people and their associations with dementia, stroke and vascular diseases.

Acknowledgements: Thanks to funders MRC Disconnected Mind (MR/M013111/1), Age UK (DCM Phase 2), Row Fogo Charitable Trust (R35865, R43412), and contributors to the LBC1936 study.

References

1. Wardlaw, J.M., Smith, E.E., Biessels, G.J., Cordonnier, C., Fazekas, F., Frayne, R., et al. Neuroimaging standards for research into small vessel disease and its contribution to ageing and neurodegeneration. *The Lancet Neurology* 2013;**12**(8):822–838.
2. Ramirez, J., Berezuk, C., McNeely, A.A., Gao, F., McLaurin, J., Black, S.E.. Imaging the Perivascular Space as a Potential Biomarker of Neurovascular and Neurodegenerative Diseases. *Cellular and Molecular Neurobiology* 2016;**36**(2):289–299.
3. Potter, G.M., Doubal, F.N., Jackson, C.A., Chappell, F.M., Sudlow, C.L., Dennis, M.S., et al. Enlarged perivascular spaces and cerebral small vessel disease. *International Journal of Stroke* 2015;**10**(3):376–381.
4. Descombes, X., Kruggel, F., Wollny, G., Gertz, H.J.. An Object-Based Approach for Detecting Small Brain Lesions: Application to Virchow-Robin Spaces. *IEEE Transactions on Medical Imaging* 2004;**23**(2):246–255.
5. Valdés Hernández, M.d.C., Piper, R.J., Wang, X., Deary, I.J., Wardlaw, J.M.. Towards the automatic computational assessment of enlarged perivascular spaces on brain magnetic resonance images: A systematic review. *Journal of Magnetic Resonance Imaging* 2013;**38**(4):774–785.

6. Ramirez, J., Berezuk, C., McNeely, A.A., Scott, C.J.M., Gao, F., Black, S.E.. Visible Virchow-Robin spaces on magnetic resonance imaging of Alzheimer's disease patients and normal elderly from the Sunnybrook Dementia study. *Journal of Alzheimer's Disease* 2015; **43**(2):415–24.
7. Wang, X., Valdés Hernández, M.d.C., Doubal, F., Chappell, F., Piper, R., Deary, I., et al. Development and initial evaluation of a semi-automatic approach to assess perivascular spaces on conventional magnetic resonance images. *Journal of Neuroscience Methods* 2016; **257**:34–44.
8. Frangi, A., Niessen, W., Vincken, K., Viergever, M.. Multiscale vessel enhancement filtering. *Medical Image Computing and Computer-Assisted Interventation-MICCAI98* 1998;:130–137.
9. Zong, X., Park, S.H., Shen, D., Lin, W.. Visualization of perivascular spaces in the human brain at 7T: Sequence optimization and morphology characterization. *NeuroImage* 2015;**125**:895–902.
10. Park, S.H., Zong, X., Gao, Y., Lin, W., Shen, D.. Segmentation of Perivascular Spaces in 7T MR Image using Auto-Context Model with Orientation-Normalized Features. *NeuroImage* 2016;**134**:223–235.
11. Greene, W.H., Hensher, D.A.. *Modeling ordered choices: A primer*. Cambridge University Press; 2010.
12. Potter, G.M., Chappell, F.M., Morris, Z., Wardlaw, J.M.. Cerebral Perivascular Spaces Visible on Magnetic Resonance Imaging: Development of a Qualitative Rating Scale and its Observer Reliability. *Cerebrovascular Diseases* 2015;**39**(3-4):224–231.
13. Lutkenhoff, E.S., Rosenberg, M., Chiang, J., Zhang, K., Pickard, J.D., Owen, A.M., et al. Optimized Brain Extraction for Pathological Brains (optiBET). *PLoS ONE* 2014;**9**(12):e115551.
14. Zhang, Y., Brady, M., Smith, S.. Segmentation of brain MR images through a hidden Markov random field model and the expectation-maximization algorithm. *IEEE Transactions on Medical Imaging* 2001;**20**(1):45–57.
15. Valdés Hernández, M.d.C., Armitage, P.A., Thrippleton, M.J., Chappell, F., Sandeman, E.M., Muñoz Maniega, S., et al. Rationale, design and methodology of the image analysis protocol for studies of patients with cerebral small vessel disease and mild stroke. *Brain and Behavior* 2015;**415**:1–18.
16. Jenkinson, M., Bannister, P., Brady, M., Smith, S.. Improved optimization for the robust and accurate linear registration and motion correction of brain images. *NeuroImage* 2002;**17**(2):825–841.
17. Pernet, C., Rand, W., Rousselet, G.. Robust correlation analyses: false positive and power validation using a new open source Matlab toolbox. *Frontiers in Psychology* 2013;**3**(606).